Leveraging Data for Green Infrastructure Performance Analysis and Prediction

By

Andrew Kurzweil

Thesis
Submitted to Department of Civil and Environmental Engineering
College of Engineering
Villanova University
in partial fulfillment of the requirements
for the degree of

MASTER OF SCIENCE, CIVIL ENGINEERING

May 2021

VILLANOVA
UNIVERSITY
College of Engineering

Andrew Kurzweil

Leveraging Data for Green Infrastructure Performance Analysis and Prediction

May 2021

Advisors:

Robert G. Traver, Ph.D., P.E., D. WRE, F.EWRI, F.ASCE ,

Bridget Wadzuk, Ph.D., and

Gerald Zaremba, Ph.D.

Villanova University

College of Engineering

Center for Resilient Water Systems

Department of Civil and Environmental Engineering

800 East Lancaster Avenue

Villanova, Pennsylvania 19085

The data presented herein were collected as part of a research initiative by Villanova University's Center for Resilient Water Systems (VCRWS) under a grant funded by the Pennsylvania Department of Transportation (PennDOT). These data are to be considered preliminary, and may not be used elsewhere except with explicit written permission from PennDOT or VCRWS. PennDOT and VCRWS make no guarantees as to the integrity of these data, which are provided for informational purposes only and are subject to change upon further review.

Abstract

In the twenty-first century, harnassing the power and abundance of environmental data has the potential to unleash a greater understand of and appreciation for the natural environment and enable better integration of the built environment by dynamically responding to the natural environment's processes. Reliably, accurately, and consistently collecting quality observations for monitoring, analysis, and future design adjustments becomes necessary when high volumes of data are able to be processed rapidly and automatically. In this thesis, I will demonstrate the need for, and benefits of, a data-oriented approach to Green Infrastructure design and analysis using the I-95 Revive project and PennDOT's SMP A site as a case study for robust monitoring networks capable of minute-by-minute measurements over a years-long span to enable better insight to the natural processes occuring in the rain garden and the potential effects on downstream hydraulics.

Acknowledgement

This thesis is a result of my studies at Villanova University and my research as a member of the Center for Resilient Water Systems' PennDOT Hydrology Team. I would like to thank my advisors, Dr. Robert Traver, Dr. Bridget Wadzuk, and Dr. Gerald Zaremba, for their endless support, for sharing their wealth of knowledge and experience, and for entertaining my continuous requests to try new things. Madhat Fares, Danielle Galloway, Shaelynn Heffernan, and Matina Shakya, my fellow graduate students, made field work a breeze and provided many hours of troubleshooting, laughs, bouncing ideas around, and more troubleshooting. The Pennsylvania Department of Transportation and AECOM's partnership were key in inspiring, funding, and critiquing our work, and I am forever grateful for their support. Last, but certainly not least, thank you to my family for providing a rich educational background and my friends for their encouragement and support along the way.

Table of Contents

List of Figures

List of Tables

List of Listings

Introduction

Modern cities are facing new and quickly emerging threats from increasingly frequent large storms, which wreak havoc on urban streams and tax urban drainage and sewer systems to dangerous levels.

Standardized Data Collection

This chapter will be based on my presentation given in April 2020 focusing on sensor network and flow measurement best practices.

Robust Data Storage

This chapter will be based on IDM paper and related work (R scripts, IDM formatter, etc...)

Performance Driven Data Analysis

4.1 Background

Green stormwater infrastructure (GSI) systems' performance has historically been difficult to measure. Most systems are designed and constructed using specifications drawn up over the last 25 or more years. While many states, including Pennsylvania, do require designs that take into consideration the pre-construction site conditions, or require a site to mimic the otherwise pre-anthropogenic environment's hydrology at the site, most do not include a post-construction monitoring plan, or predefined performance metrics that can be used to quantify a location's response to storm events over its lifespan. The lack of post-construction monitoring and analysis poses a major roadblock to improving recommendations for the design process that could lead to higher GSI longevity, lower the risk of GSI failure or under-performance, and creating uniform standards for GSI comparisons between geographically distinct sites or projects. Even when these monitoring requirements are in place, diverse site conditions, geographies, and climates necessitate a standardized framework for quantifying performance and comparing between potentially vastly different sites. This chapter outlines proposed key performance indicators (KPI) unique to infiltration-type rain garden GSI by looking at historical data for a site located in PennDOT's GR2 section of the I-95 Revive project (referred to as SMP A henceforth). These robust monitoring and analysis techniques will lead to consistent results that can be applied across many sites while ensuring that outside factors do not influence performance measurement results. A standard approach to analysis will open the door to suggested improvements for designs and further exploration of GSI's importance to more sustainable urban environments.

4.2 Recession Rate

Recession rate, or the change in depth of water ponded over time, is a potential key performance indicator (KPI) for GSI because it provides an easy to measure proxy for soil health. Soil health, in the context of GSI infiltration, is defined as a lack of compaction, clogging, or other infiltration inhibiting issues (Sokolovskaya et al., 2021). These properties of soil are heavily influenced by saturation level, which is a proxy for hydraulic conductivity and the shape and location of a soil-water characteristic curve (SWCC). Hydraulic conductivity of soil is the property that defines the ability of

soil to pull water from the surface and through the soil column. The SWCC defines how a given soil responds to varying saturation levels, and the suction force applied to water in contact with the soil. Saturation of soil occurs when all the void space is filled with water and the movement of water through the soil column reverts to a gravity driven system that is largely influenced by soil characteristics. Saturated soil generally has the lowest hydraulic conductivity among the range of all volumetric water content (VWC) values possible for that given soil (Eyo et al., 2020). Different soils can have significantly different hydraulic conductivity ranges, and engineered soil with favorable properties (higher hydraulic conductivity) is generally specified for GSI design where infiltration is a desired treatment method.

By calculating a water level differential across consecutive data records, the change in water level can be used to determine periods of increasing or decreasing volume in the ponded storage. When negative, recession is occurring, provided there is no rainfall or inflow happening simultaneously. Additionally, the current water level must be confirmed as being below the overflow point of any outlet structures to ensure, as much as possible, that the recession rate can be attributed solely to infiltration. The magnitude of recession is important because it indicates the state of the GSI, or how saturated the soil is. Larger recession rates indicate a faster drawdown of the water level, while smaller values indicate potential saturation conditions or under-performance. Comparing average recession rates calculated over the duration of a storm to other simultaneously recorded atmospheric and GSI state data shows the relationships that have the most significant impact on GSI performance. Changes in the recession rate over the period of a storm, or between the average recession of storms over a longer period of time, indicates changes in the soil health.

Similarly, the drying rate of the soil may be calculated by finding the average time lag between the end of ponding at the surface and the drop in saturation at a known depth, or between the drop in saturation at two separate depths. Using soil moisture probes at 10, 35, and 60 cm allows the calculation of an average rate of the descent of saturation conditions as the soil begins to recover following ponding. This subsurface drying rate should remain consistent between events of different sizes, so long as the soils reach saturation.

These relationships are complicated by several factors, namely the timing and size of an event, the state of the GSI at the beginning of an event in both a geomorphology and atmospheric scope, and the interaction between the two. The timing and size of a storm event, which can be best described by a combination of time of year, hyetograph, and the length of time since the last storm event, are important because these play the largest role in determining how the pre-storm state of the GSI

will react to specific conditions. The starting state of the GSI is important because it necessitates an adaptable baseline against which analyze performance. For example, a storm taking place during early spring in the Philadelphia, PA region could have a wide range of pre-storm soil moisture, air and water temperatures, or plant growth conditions, to name a few. Additionally, the fact that suction head is highest when the soil is dry (Eyo et al., 2020), means that infiltration loss is greatest at the beginning of an event, no matter the specific initial conditions, because that is when the soil is driest.8/ This confounding relationship means that the most consistent means of comparison will be between the most steady parts of a storm event. For recession rates, this means looking at the trailing end of a storm, when there is no inflow, ponding level has reached its peak, and the soil has reached saturation. Allowing the GSI to reach a steady state means that comparisons will be made strictly between the soil's infiltration performance, without the influence of a specific storm event's timing characteristics.

The following sections discuss the data used to support these hypotheses, and show that recession rate and soil drying rate can be used as proxies for soil health and extended to overall GSI performance. The data were collected with support from the Pennsylvania Department of Transportation (PennDOT) and AECOM as part of the I-95 Revive project. The site monitored is SMP A, a linear infiltration type GSI rain garden located on the southeast side of I-95 North between Frankford Avenue and Shackamaxom Street. The site includes two ponding and overflow locations (B1 and B2), three inlets piped from the adjacent raised highway bed, and two check dams splitting the garden into roughly equal thirds (upstream, gabion, downstream).

4.3 Data and Modeling

Data collected is 5 minute averages of 1 minute records (values are measured every minute and stored every 5 minutes as the average of the previous 5 values). This data resolution captures enough detail without producing an overwhelming number of data records. The following outlines relationships determined from data collected at SMP A over a period of interest of nearly 3 years (May 2017 - November 2020). To better synthesize the data collected, summary statistics for predefined hydrological events are generated based on either a total amount of rainfall followed by a minimum dry time (typically 6 hours), or based on characteristics of other variables of interest - namely ponding and soil moisture values.

4.3.1 Event Definition

Using clearly defined rules to identify events is the first step to generating meaningful summary statistics that are applicable across time and space, and useful for comparing GSI with dissimilar properties. In a GSI context, events are storms that result in a measurable quantity of precipitation, sometimes with a lower bound of 0.5 inches, or 12.7 millimeters, depending on the analysis requirements. Events with less than 0.5 inches of rainfall typically do not have a pronounced impact on GSI, and so they have typically been disregarded unless otherwise noted. For this analysis, a 'standard,' or 'normal' storm event begins when rainfall is first recorded and continues until 6 hours after the last observed rainfall. This means the absolute minimum event duration is 6 hours, and any periods without rainfall of less than 6 hours are continuations of the same storm event. This definition is used as the standard both for generating storm summary data in monthly reports to PennDOT and for all analyses henceforth that do not directly involve soil moisture observations. During the period of interest, there were 414 observed standard events with a mean duration of 12.2 hours, a median of 9.5 hours, and a standard deviation of 7.5 hours. The data are highly right-skewed, with a maximum of 52.2 hours, and appear to follow a roughly chi-square distribution (Figure 4.1).

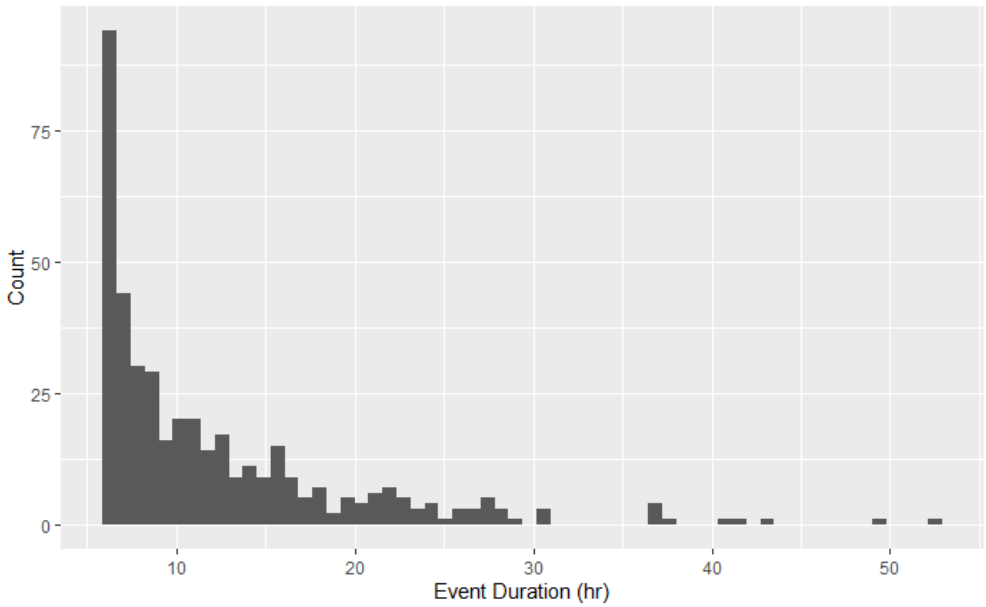

Figure 4.1: Distribution of event lengths.

Events are distributed throughout a Gregorian 365-day year approximately uniformly, as seen in Figure 4.2, although there are some notable event clusters in both late spring (around ordinal day 150), and during hurricane season (after ordinal day 200). There are notably fewer events during the winter months, but this is likely due to the instrumentation's lack of sensitivity to snowfall, which is a somewhat common occurrence during Philadelphia's winter months.

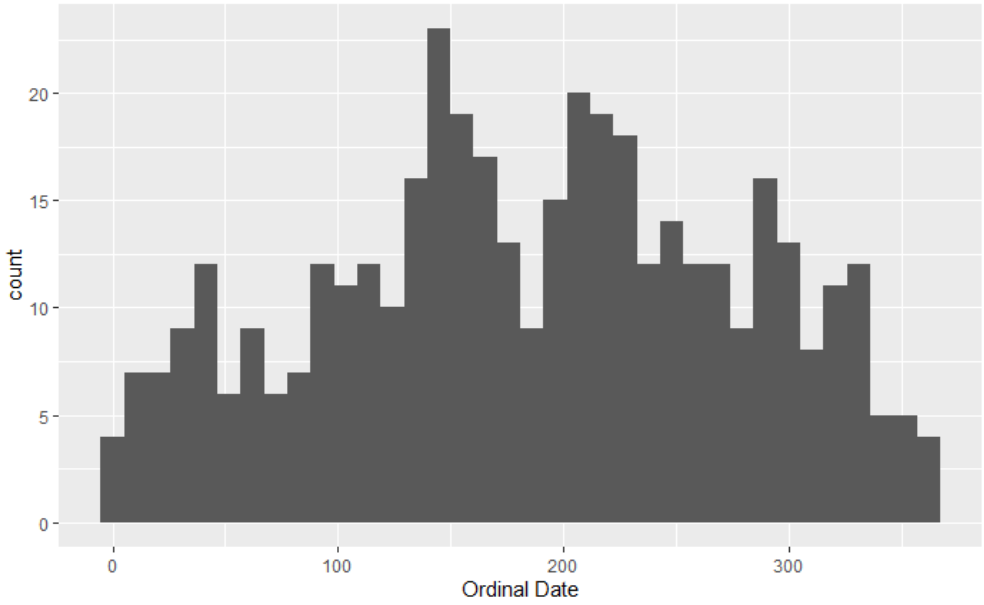

Figure 4.2: Distribution of event ordinal dates.

For events involving soil moisture, due to the prolonged nature of soil moisture's response to storm events, a modified approach is necessary. Soil moisture, and by extension ponded water atop saturated soils, take longer than 6 hours to recover after storms of interest (>0.5 inches of rain). To define events for these analyses, both rainfall and soil moisture levels are considered. As before, an event begins with the first observed rainfall. However, the end of the event is defined by a minimum event time (6 hours) as well as a threshold ponding level or soil moisture level (either may be used, depending on the type of analysis being performed). A simple moving average of the number of steps comprising the minimum event duration (in other words, the data interval - 5 minutes -

divided into the minimum event time of interest) provides a window into the past or the future at a given time step, and can be used to define an event as follows:

$$\begin{aligned} Event = \{ & A = [moving\_average(rainfall, Q/P) > 0], \\ & B = [moving\_average(rainfall, Q/P) == 0 \\ & \cap\, moving\_average(K, Q/P) < R] \} \end{aligned} \tag{4.1}$$

where A is an indicator for the beginning of an event, B is an indicator for the end of an event, Q is the minimum event duration, P is the observation interval, R is a threshold value, and K is the variable of interest. Timestamps falling between successive A and B values are assigned a unique, random string of 8 characters generated from the first timestamp in the series. The distribution of these specialized events is similar to that of the standard events above, although there are generally fewer of them due to increased strictness of the criteria.

4.3.2 Temperature Dependence

The weather station at SMP A records air temperature, and each pressure transducer (PT) records the temperature of water in which it is submerged. The two types of temperature are highly correlated, and for the purpose of this analysis, only water temperature will be considered. Testing for variations in recession rate across the range of observed water temperatures shows a relationship that is largely linear (Figure 4.3).

Calculating the average recession rate on a storm event basis and examining the distribution of these recession rates separated into bins based on average water temperature (Figure 4.4) over the duration of the event shows a clear trend indicating higher recession rates at higher water temperatures. Five bins were chosen to give n > 20 for most bins. The lowest bin ((-0.05,5.83]) has only 7 events but follows an identical trend to the upper four bins. This aligns with several physical and hydrologic models, namely that warmer water is less viscous and flows easier, especially through the soil (Emerson and Traver, 2008), such that, since warmer soils contain warmer water, there is less internal resistance to flow by the soil at warmer temperatures. This means that GSI performance can be expected to increase during warmer months, both due to increased infiltration capacity and increased water uptake and evapotranspiration by the plant mass [CITE]. Furthermore, it has been shown that soils which have experienced multiple freeze-thaw cycles have higher values of saturated hydraulic conductivity due to the formation of internal ice crystal structures within frozen soils

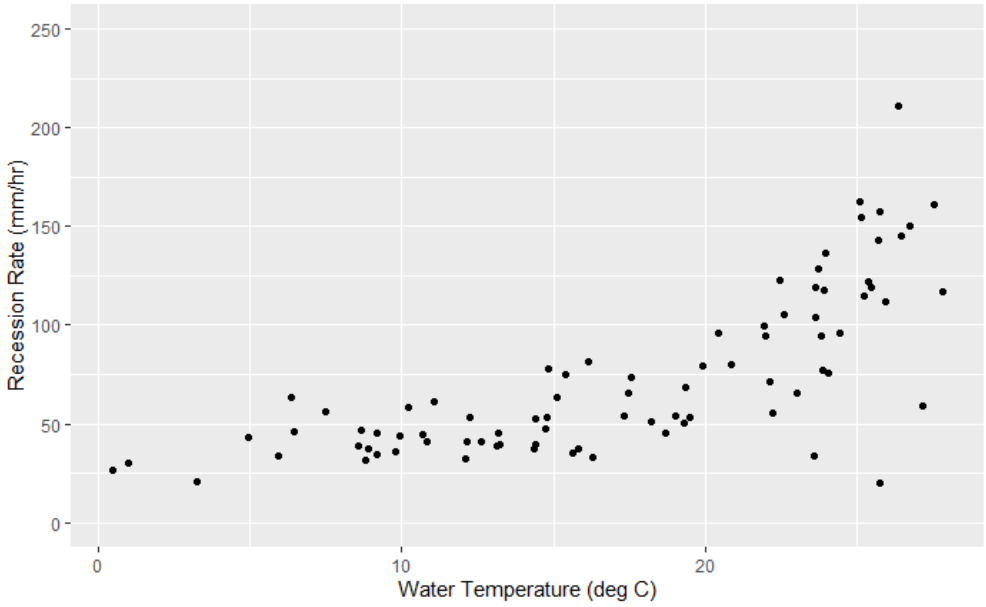

Figure 4.3: Average water temperature vs Recession Rate for SMP A storm event.

(Asare et al., 1999), which can expand pore space and increase the "development of macroscopic cracks and microscopic voids." Therefore, soils that experience freezing conditions followed by warm conditions, as is typical in a climate with a distinct harsh winter season, can expect to see a natural "loosening" of the soil via the creation of these additional void spaces.

4.3.3 Atmospheric Influences

Both relative humidity (RH) and barometric pressure, both recorded in a similar fashion to air temperature at SMP A, showed no significant relationship with recession rate. Comparing the average recession rate to RH bins and pressure bins, similar to the approach taken in the previous temperature analysis, shows no correlation between different values for these variables as compared to the average recession rate (Figure 4.5 and 4.6).

This means that GSI performance is not dependent on these atmospheric variables, which largely only impact the soil-air interface. The lack of relationship between the atmosphere and sub-surface infiltration mechanics is expected, since the soil contains enough mass to prevent significant influence from the relatively fast-changing atmosphere.

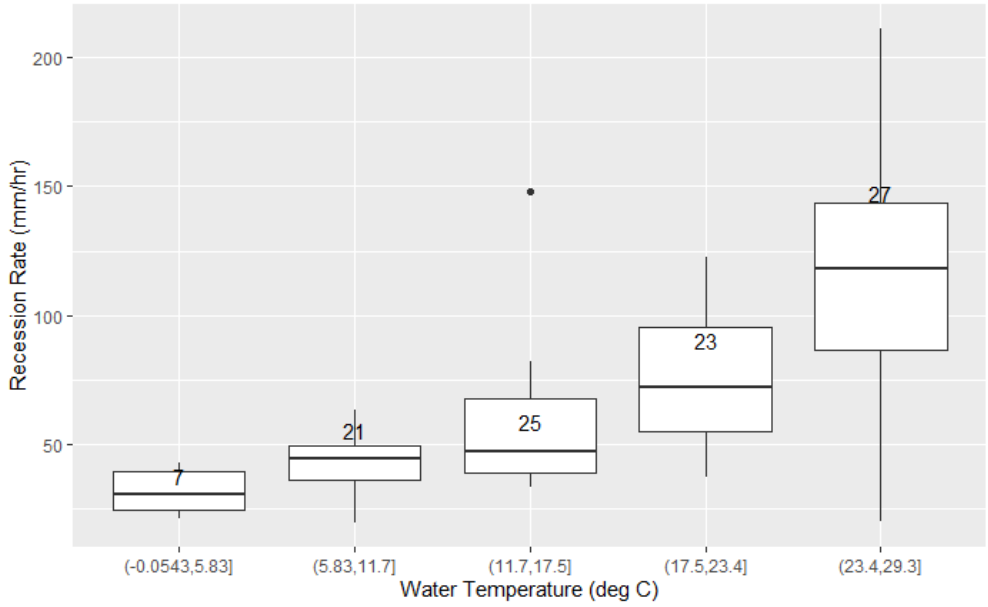

Figure 4.4: Average water temperature vs Recession Rate, separated into bins.

4.3.4 Ponding Depth Influence

The amount of water collected in the rain garden similarly has no effect on the rate of recession. This runs contrary to expectations that greater head pressure at the soil-ponding interface would lead to higher recession rates. The rate of recession is consistent across nearly the entire ponding depth range (Figure 4.7). The lack of correlation, while surprising, could be due to the fact that sufficient sub-surface hydrostatic pressure exists such that it cancels out the head pressure seen at typical ponding depths of up to a maximum of less than 1 meter. The data support this conclusion, however, since a simple linear regression between recession rate and ponding depth yields an R-squared value of just 0.0027, meaning just 0.27% of the variation in recession rate is due to variations in ponding level. While the slope estimate and F-statistic for this model are both significant at the 0.05 level, the low R-squared value means the model is only predicting the mean recession rate.

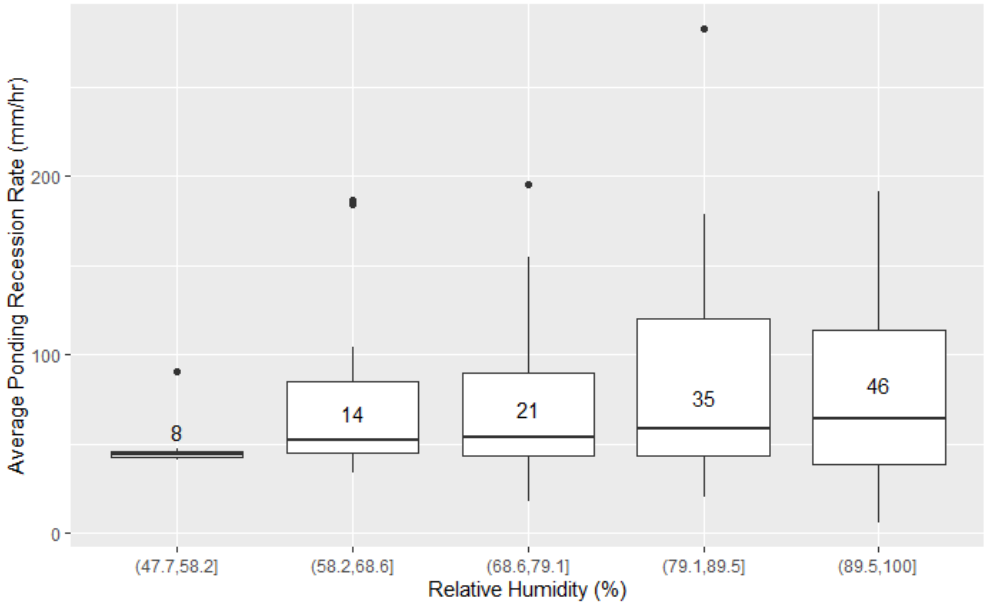

Figure 4.5: Average Relative Humidity vs Recession Rate

4.3.5 Comparisons to Ordinal Day

Another explanation of the variability in recession rate is the more simple ordinal day approach. This suggests a seasonal variation to GSI performance that is largely independent of temperature, despite temperature being strongly correlated. To investigate this, a seasonal trend must be fit the to the data and subtracted away in order to determine if the adjusted recession rates remain as variable as the non-adjusted data.

4.3.6 Extension to Drying Rate of Soil

Similar to the recession of water ponded on the surface of the garden, the recession of water within the soil column reflects the soil health of the site. Measuring the soil moisture values for the duration of a storm event produces a curve that typically looks like Figure 4.8. The soil moisture curve can typically be expected to respond with a sharp upward jump, 5-20 minutes in length, at the beginning of the storm event's inflow. During this period, the initial runoff is saturating the soil, with the wetting front moving mostly in the vertical direction, driven by suction head. The soil

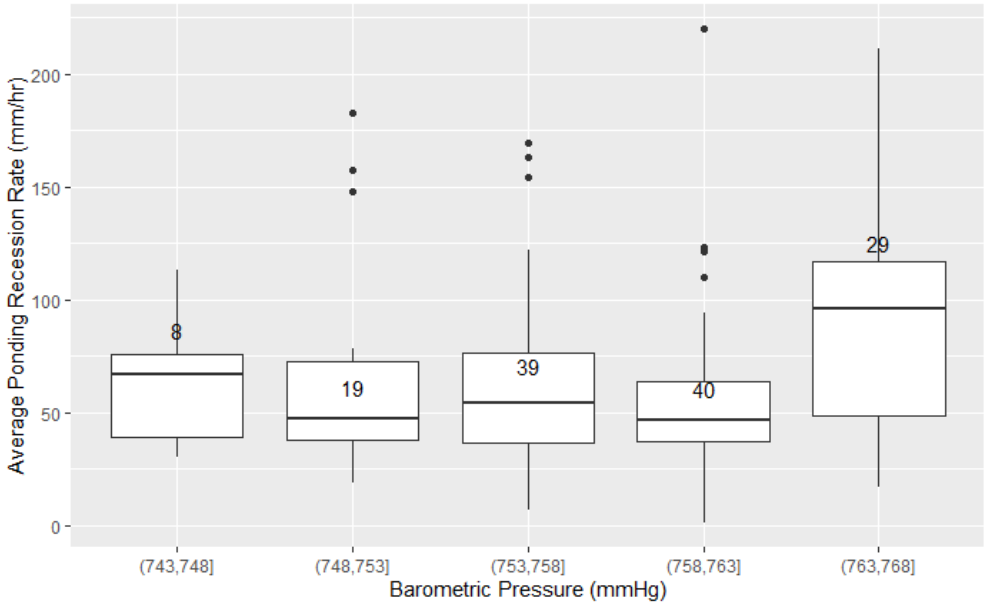

Figure 4.6: Average Barometric Pressure vs Recession Rate

moisture curve has been characterized with a series of 7 points in work completed by Matina Shakya, PhD Candidate working on soil moisture measurements for VCRWS/PennDOT. The following is an extension of the first four of these points. The beginning and end of this positive jump are identified as points 'A' and 'B', respectively. Point A is typically below 0.40, or 40% volumetric water content (VWC), while point B is typically between 0.45 and 0.50, or 45-50% VWC. Soil moisture levels remain at saturation conditions for the duration of ponding, due to continuous infiltration, eventually leading to the full recession of ponded water. The reduction in volume from the system due to evaporation, evapotranspiration, or any other means is assumed to be negligible compared to infiltration during this period. Recession of the saturation conditions within the soil behave much like the initial wetting front, but in reverse as water continues to percolate downwards through the soil column. The trailing limb of the saturation curve can be identified by two additional points, 'C' and 'D' in Figure 4.8, identified as the drop off point and inflection point of the soil moisture curve, respectively.

This process is also slightly temperature dependent, as seen in Figure 4.9, which shows the event average ponded water temperature plotted against the mean time in hours between the end of ponding and the end of saturation at the 10cm soil moisture probe.

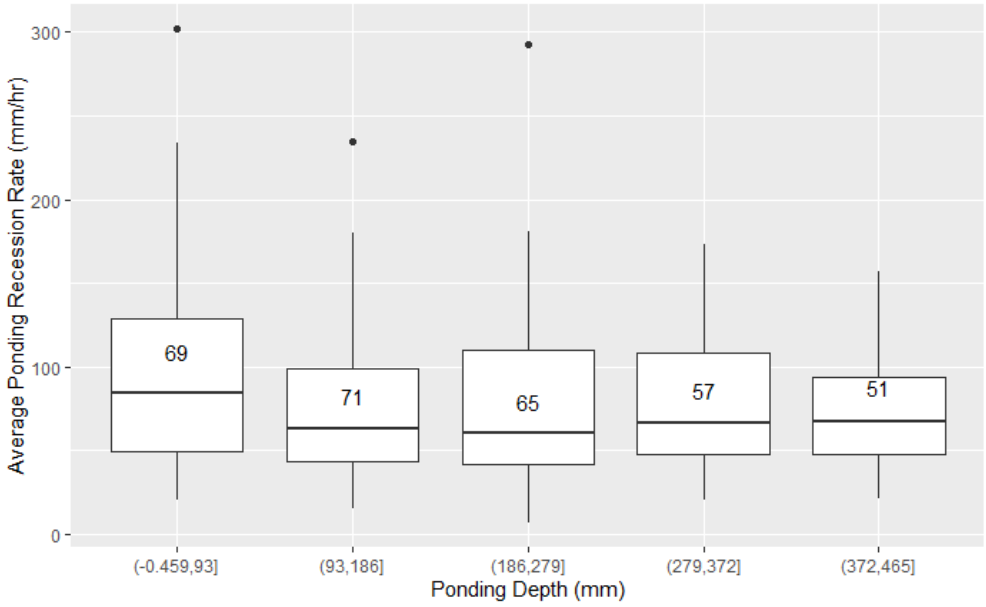

Figure 4.7: Average Ponding Depth vs Recession Rate

The calculation of this metric is slightly more complicated than raw recession rate of the ponded water presented earlier. The inflection points A, B, C, and D are calculated as the 4 primary peaks in the absolute value of the first differential of the soil moisture data:

$$InflectionPoint\{A, B, C, D\} = localmax(|\theta_i - \theta_{i-1}|)_j \tag{4.2}$$

where i = 1,2...n for n observations in a given storm and where j = 1,2,3,4 corresponding to A,B,C,D. These points are easily calculated using the 'findpeaks' function from the R package 'pracma' (`pracma::findpeaks()`). The function takes a vector of data, the absolute value of the differential soil moisture data applicable to one storm event in this case, and returns the indices of the requested number of local maximums (4 in this case), which can be put in order with a simple sort. Depending on the specific values of soil moisture seen during an event, the four indices may be returned in any order, largely based on the magnitude of difference between any two given points. The basic premise only requires that the four points are properly identified, as they can be easily sorted to identify their correct placement. However, due to the highly variable pre-event state of the GSI, storm events that begin with saturated VWC values (>0.44 VWC) often misidentify some or all of these points, so these events have been disregarded in the context of this analysis. This results in

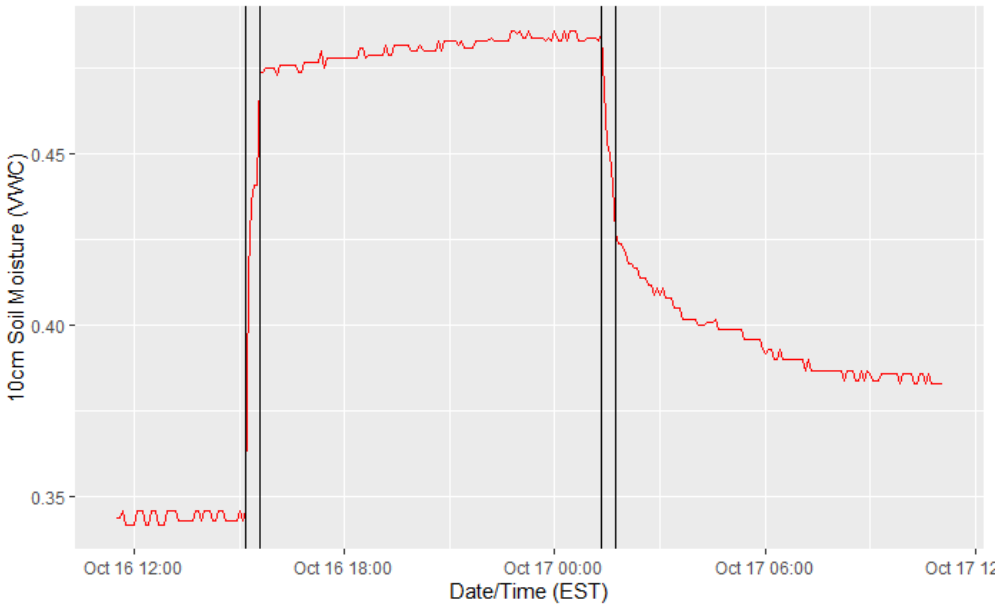

Figure 4.8: Typical soil moisture curve. Vertical black lines denote points A, B, C, and D from left to right, respectively.

76 valid events from the period of interest, which are essentially a subset of the standard events, quantified with different ending criteria. For each event, the rate of drying for the 3 zones between the surface and the three soil moisture sensors at progressively deeper placements is calculated as distance/time. Figures 4.10, 4.11, and 4.12 demonstrate that this rate can be expected to fall within 0-5 cm per hour. The 95% percentile falls at 9.5 hours between 10 and 35cm (approx 2.63cm/hr), and 7.4 hours between 35 and 60cm (approx. 3.37cm/hr), meaning 95% of events can be expected to exhibit drying rates higher than this. The distribution does not display correlation with water temperature (Pearson correlation 0.047, p-value 0.34), and has remained consistent over time, as displayed in Figure 4.13.

4.3.7 Regression

Using multiple linear regression, a numeric relationship between the recession rate and pond temperature, max pond depth, ponding duration, total rainfall, and average rainfall intensity can be determined. The expected value of this relationship can determine if a GSI system is functioning nominally. Values that are outside the expected relationship boundaries are cause for concern, and a

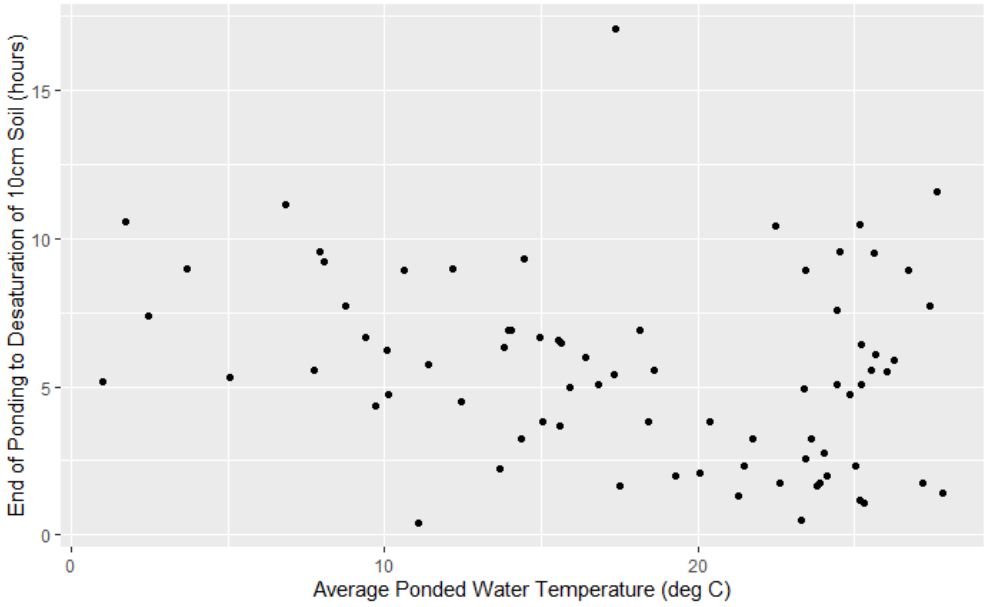

Figure 4.9: Average Water Temperature vs Time to Desaturation at 10cm.

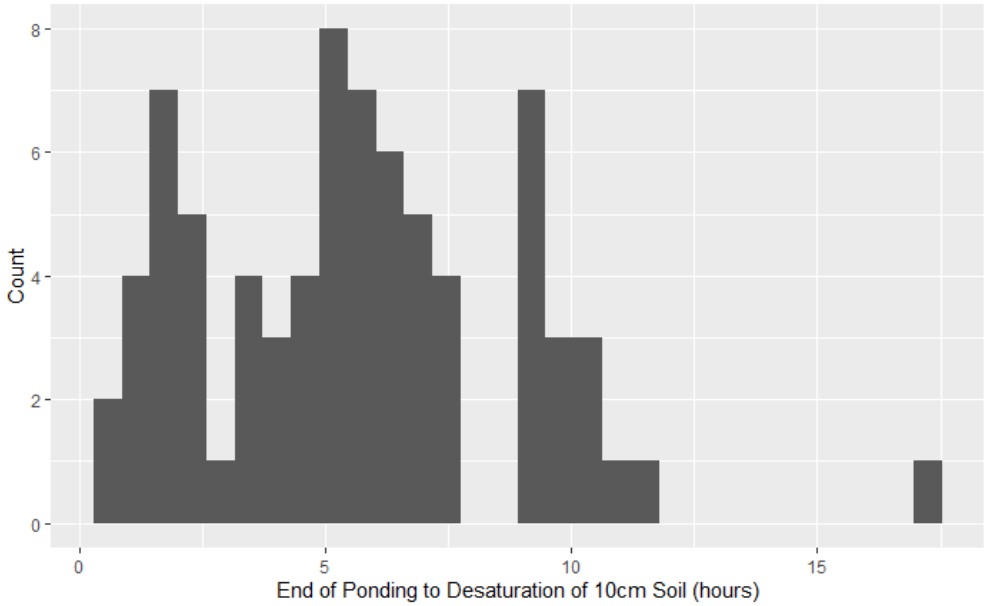

Figure 4.10: Time to Desaturation between end of ponding and 10cm.

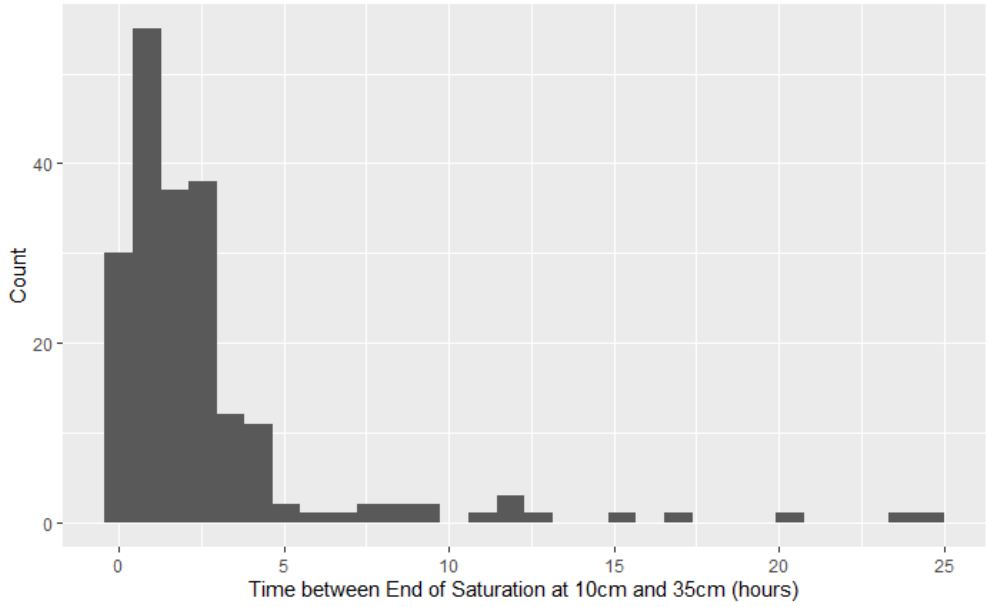

Figure 4.11: Time to Desaturation between 10 and 35cm.

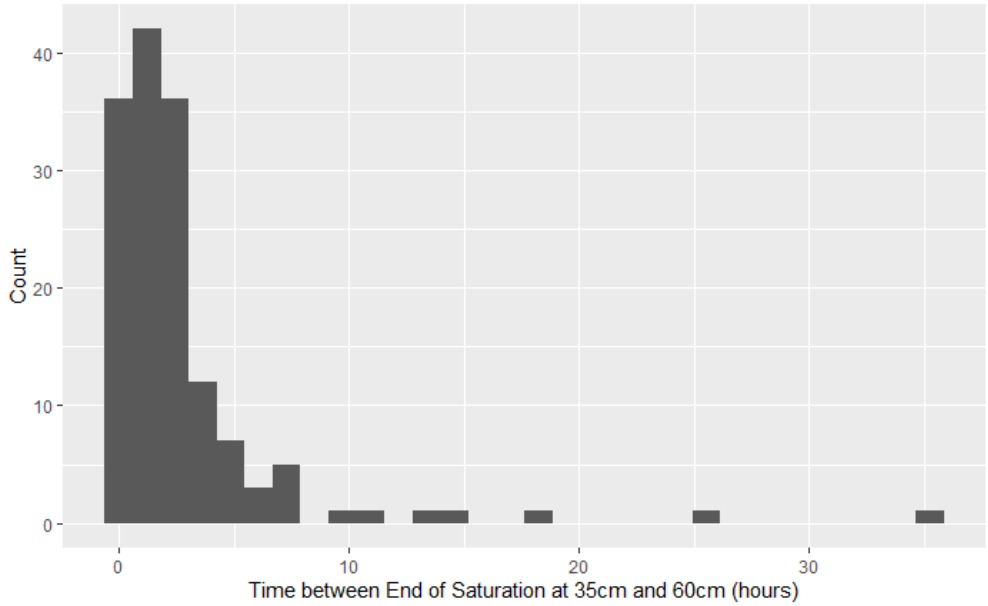

Figure 4.12: Time to Desaturation between 35 and 60cm.

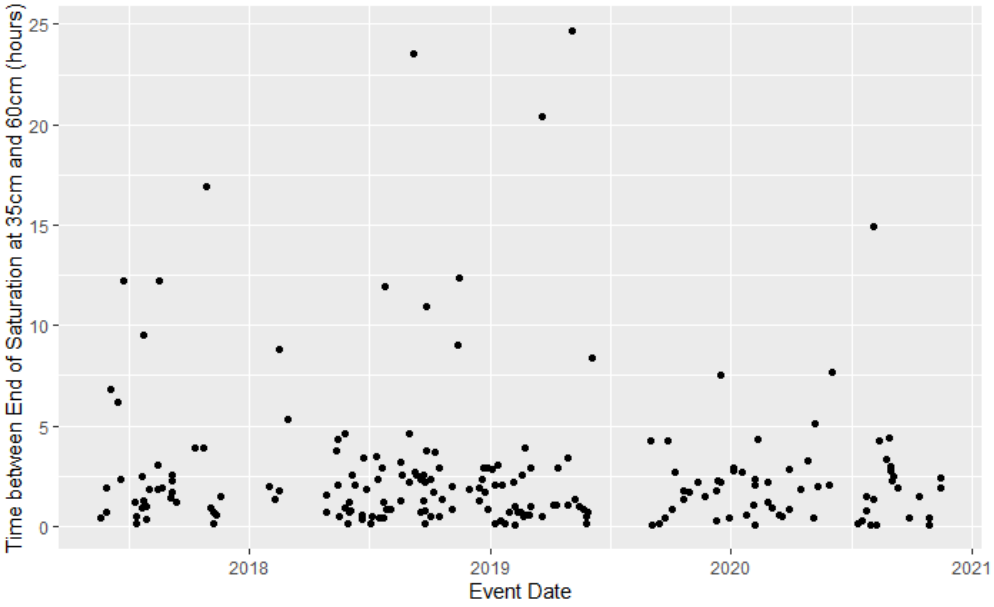

Figure 4.13: Event Date vs Drying Time between 10 and 35cm.

trend of values outside the norm would indicate that maintenance or further evaluation of the system is required. While the numbers presented here are specific to PennDOT's SMP A, this approach, and indeed the entire scope of data collection, storage, and analysis would be of tremendous value to any system or group of systems with similar properties.

Regressing the following parameters onto ponding recession rate (mm/hr) results in the listed effects (Table 4.1), which results in Equation 4.3, the relationship for water temperature, pond depth, ponding duration, total rainfall, and average rainfall intensity with respect to ponding recession rate. The R-squared value is 0.9023, with an F-statistic (significance test) of 312.1 on 5 and 169 degrees of freedom (p-value = $< 2.2e-16$), indicating the partial slopes ($\beta_1 \dots \beta_5$) are not equal to 0. There are, however, normality concerns, as demonstrated by the normal quantile-quantile plot (Figure 4.14), which shows a departure from linearity beyond ± 1.5 quantiles. This is somewhat expected, as the data are not normally distributed, so an additional nonparametric test is required to confirm the trend seen. The relationship lacks an intercept because the mean response is expected to be 0 mm/hr, corresponding to no ponding recession when all other variables are also 0.

$$y = \beta_1 * 0.2384 + \beta_2 * 0.11721 - \beta_3 * 0.98104 - \beta_4 * 0.1821 + \beta_5 * 0.3771 \tag{4.3}$$

Table 4.1: Ponding recession rate regression results.

	Coefficient	Estimate	Std. Error	t value	Pr($>|t|$)
β_1	B1 pond mean temp (°C)	0.238352	0.085110	2.801	0.005697
β_2	B1 pond max depth (mm)	0.117213	0.005684	20.622	<2e-16
β_3	B1 ponding duration (hr)	-0.981035	0.224939	-4.361	2.24e-05
β_4	Total Rainfall (mm)	-0.182069	0.063980	-2.846	0.004980
β_5	Average Intensity (mm/hr)	0.377106	0.110401	3.416	0.000797

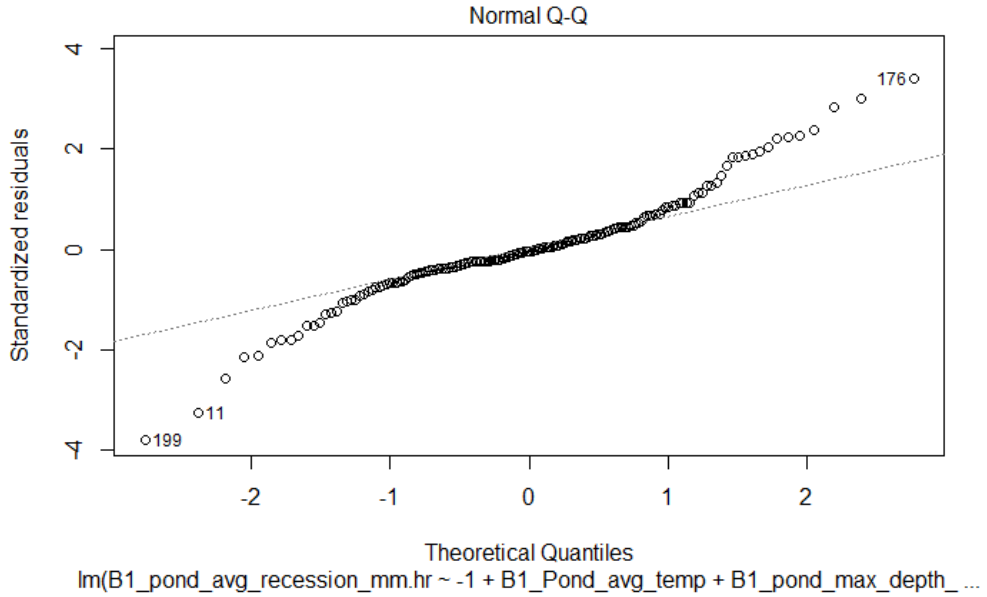

Figure 4.14: Normal Q-Q plot for ponding recession regression.

This model was chosen for its high R-squared value, which reflects the percent of variation in the response (recession rate) explained by the total variation in the model parameters, as well as its overall significance (high F-statistic with low p-value). Other models considered included some combination of the final parameters, water temperature, event duration, and ordinal day.

The model is not without its shortcomings, however, and corrections for the departures from normality of the training data are necessary. The Kendall seasonal trend statistic, τ, tests for seasonal trends in monotonic, nonparametric data. The statistic is a ratio of the probabilities of the observed order of the data to that of a different ordering. That is, assuming two variables (X and Y, for example) are independent, the expected value of τ is 0, as the likelihood of the observed ordering

Table 4.2: Kendall seasonal trend results.

Variable	Kendall τ	p-value
B1 pond mean temp (°C)	0.1226526	0.001711
B1 pond max depth (mm)	0.9150601	<2.2e-16
B1 ponding duration (hr)	0.8294355	<2.2e-16
Total Rainfall (mm)	0.5483617	<2.2e-16
Average Intensity (mm/hr)	0.4102984	<2.2e-16

is equal to that of any other ordering for two independent series Abdi, 2007. Calculating τ for comparison between B1 recession rate and the variables found in the regression equation 4.3 results in the values found in Table 4.2. All the relationships are significant enough to reject the claim that the pairwise comparisons are independent, suggesting the trends observed, and by extension their inclusion in a normal multiple regression, are significant, despite the lack of normality.

4.4 Results and Discussion

The methods described here attempt to evaluate methods for comparing storm events across time, space, or both. Using these KPIs to address a system of GSI performance across an entire region will enable insights into long term design successes, and early detection of system errors. The data have shown that performance is most highly impacted by temperature, which oscillates with an annual seasonal period. GSI can generally be quantified in terms of recession and drying rates for ponding level and soil moisture, respectively. Higher rates for each indicate faster transfer of water into the subterranean water table, and faster reduction in soil moisture that will lead to better preparation for the next storm. In general, average infiltration rates between 40 and 120 mm/hr can be expected, depending on time of year and water temperature. Average drying rates centered around 9.5 cm/hr can be expected, although this value would be expected to vary from GSI to GSI based on soil design criteria. These statistics are not dependent on GSI parameters such as surface area, loading ratio, or number of inlets or outlets. Therefore, the statistics can be calculated for any GSI system, or part of a system, to determine if infiltration rates and recovery rates fall within the expected range. Thanks to the few parameters needed, namely ponding depth and soil moisture level, few sensors are necessary, keeping costs for this kind of monitoring low, making it accessible to be deployed at a larger number of sites, or at multiple locations within a single site. While this work intentionally does not address spatial variability within a single site for infiltration or drying

rates, the data collected are assumed to represent the average conditions throughout SMP A, and the same assumption would be valid for the statistics calculated at other sites in a similar manner.

Because these two rates are affected by conditions both above and below the soil surface, they provide an acceptable proxy for soil health. Infiltration rate is shown to be affected by temperature, and could be reduced by clogging of the soil surface, or compaction of lower soil layers, leading to reduced rates. Similarly, drying rate is shown to be consistent across a wide variety of GSI conditions, and could be adversely affected by changing soil properties that make the GSI function less efficiently.

Conclusion

Bibliography

Abdi, Hervé (2007). “The Kendall Rank Correlation Coefficient”. In: *Encyclopedia of Measurement and Statistics* (cit. on p. 20).

Asare, S. N., R. P. Rudra, W. T. Dickinson, and G. J. Wall (1999). “Effect of freeze-thaw cycle on the parameters of the green and ampt infiltration equation”. In: *Journal of Agricultural and Engineering Research* 73.3, pp. 265–274 (cit. on p. 10).

Emerson, Clay H. and Robert G. Traver (2008). “Multiyear and Seasonal Variation of Infiltration from Storm-Water Best Management Practices”. In: *Journal of Irrigation and Drainage Engineering* 134.5, pp. 598–605 (cit. on p. 9).

Eyo, E. U., S. Ng’ambi, and S. J. Abbey (2020). *An overview of soil–water characteristic curves of stabilised soils and their influential factors* (cit. on pp. 5, 6).

Sokolovskaya, Natalya, Ali Ebrahimian, and Bridget Wadzuk (2021). “Modeling Infiltration in Green Stormwater Infrastructure: Effect of Geometric Shape”. In: *Journal of Sustainable Water in the Built Environment* 7.2, p. 04020020 (cit. on p. 4).